Optimal Use of Harvested Solar, Hybrid Storage and Base Station Resources for Green Cellular Networks

Po-Han Chiang, *Student Member, IEEE*, Ranjini B. Guruprasad, *Student Member, IEEE*, and Sujit Dey, *Fellow, IEEE*

***Abstract*—Renewable energy (RE) is a promising solution to reduce grid energy consumption and carbon dioxide emissions of cellular networks. However, the benefit of utilizing RE is limited by its highly intermittent and unreliable nature, resulting in low savings in grid energy. To minimize the grid energy cost, we propose to utilize data buffer of user equipments as well as energy storage at the base station (BS) to better adapt the BS resource allocation and hence its energy consumption to the dynamic nature of RE. We consider the scenario of downlink orthogonal frequency division multiple access networks with non-ideal hybrid energy supply. To jointly optimize the energy consumption and the quality of service (QoS) of users, we adopt the weighted sum of users' utility of data rates and grid energy consumption as our performance metric. We propose a low-complexity online control scheme based on Lyapunov optimization framework. The proposed technique can provide asymptotically optimal performance bound without requiring the stochastic distribution information of RE arrival and channel state condition. The experimental results demonstrate the ability of the proposed approach to significantly improve the performance in terms of grid power consumption and user QoS compared with the existing schemes.**

***Index Terms*—Lyapunov methods, energy storage, solar energy, stochastic optimal control, mobile communication.**

I. Introduction

THE PROLIFERATION of mobile traffic will lead to drastically increasing energy consumption in future cellular networks. The total energy consumption and carbon dioxide equivalent (CO_{2e}) emission of mobile cellular networks globally for 2020 has been estimated to more than 120TWh and 179 million tons (Mt) [2]. According to [3], base stations (BSs) consume 80% of the total power in cellular networks. Therefore, the need to reduce the grid power consumption of the BSs is crucial for energy-efficient cellular networks. There has been significant research of energy-efficient BSs [4], ranging from physical layer approaches involving power and spectral resource allocation [5], [6] and RF chain switching [7] to network level techniques wherein active BS selection and user association [8] is performed. In addition to the above techniques focusing on reduction of BS energy consumption, powering BSs with renewable energy (RE), which may increase BS energy consumption while reducing grid energy consumption of BSs, is a promising solution [9], [10]. Though the last few years have seen tremendous growth in the use of RE in several commercial and industrial sectors, its adoption in cellular networks has been limited. The primary challenge in utilizing RE energy for BSs is the highly intermittent, unreliable and variable nature of RE availability across time and space, leading to mismatch between RE generation and loads [11]. In this paper, we will mainly focus on solar energy, however, our insights and proposed approach will apply to wind and other intermittent RE sources.

One approach to overcome the challenges of intermittency and variability of RE availability is the use of high capacity batteries [12]. However, high CAPEX of such systems limits the economic viability for operators and growth of RE-powered BSs. Therefore, using RE in conjunction with grid energy (i.e., hybrid energy supply (HES)) is a viable approach to save grid energy [13]–[17]. The other challenge is the non-ideal behavior of batteries. For example, lead-acid batteries are widely used in telecommunication power systems as backup power supply and energy storage. From [12], the efficiency of lead-acid battery depends on the charging/discharging rate and state of charge and is lower than 75%. Batteries are assumed to be ideal in most of the previous green communication studies [13]–[16]. In this paper, we will incorporate the non-ideal characteristic of batteries and propose the corresponding charging and discharging decision.

In our preliminary work [1], we propose a RE-aware technique to adapt time resource of the BS and data buffers at user equipments (UEs) depending on the amount of harvested RE at the BS, channel condition and buffer level of UEs. We have demonstrated that the technique increases the utilization of RE and hence decreases the grid energy consumption without requiring energy storage. However, there are two main limitations: 1) Excessive solar energy is wasted if the harvested solar energy is larger than maximum power consumption of BS or data buffer of all users is full, 2) depletion of UE data buffer

Manuscript received August 15, 2017; revised January 31, 2018 and April 18, 2018; accepted April 30, 2018. This work was supported by National Science Foundation under Grant CNS-1619184. This work has appeared in part at the 26th IEEE Annual International Symposium on Personal, Indoor, and Mobile Radio Communications (PIMRC) [1]. The associate editor coordinating the review of this paper and approving it for publication was J. S. Thompson. *(Corresponding author: Po-Han Chiang.)*

The authors are with the Department of Electrical and Computer Engineering, University of California at San Diego, La Jolla, CA 92037 USA (e-mail: pochiang@ucsd.edu; rgurupra@ucsd.edu; dey@ece.ucsd.edu).

Digital Object Identifier 10.1109/TGCN.2018.2834519

may limit the ability to adapt the BS resource and hence grid energy saving. Therefore, we propose the use of energy storage to complement the RE-aware BS resource allocation technique in this work.

In this work, our objective is to minimize grid energy consumption of BSs as well as maximize QoS of users while optimally utilizing harvested solar power. The focus of the proposed approach will be to modulate BS energy consumption with the use of both energy storage at the BS and data storage of the UEs in order to mitigate the mismatch between harvested solar energy and BS energy consumption. Though the proposed approach is applicable to any application that utilizes data storage of users, we consider the problem for video download/streaming, which will play a large proportion of mobile traffic and hence the BS energy consumption.

A. *Related Work*

Various relevant recent work that address the use of renewable energy to minimize grid energy in wireless cellular communication are briefly discussed below. Gong *et al.* [13] and Tutuncuoglu *et al.* [17] focus on a single BS-UE link of the HES BS and propose an optimal BS resource allocation technique using the two-stage water filling (WF) policy to minimize grid energy consumption. Unlike the above techniques which consider only a point-to-point link with fixed transmission rate requirement, our approach adapts transmission rate and BS resource allocation of multiple BS-UE links. Farooq *et al.* [18], [19] propose an energy cooperation scheme where BSs trade and transfer energy via smart grid based on RE availability and traffic load. However, the technique requires BSs to be fully connected with two-way power grid to transfer energy while we focus on shaping the power consumption of the BS to realize grid energy reduction. BSs with Non-direct energy transfer schemes are proposed to minimize the grid energy cost either by traffic offload [14] or cognitive spectrum sharing [20]. However, these approaches require frequent inter-cell coordination to adapt cell size or spectrum sensing while our technique is applicable to a single cell and do not require to change cell size. Approaches have also been developed for cellular networks with HES which also use battery storage [13]–[16]; however, the above approaches assume the battery to be ideal, while our work does consider battery imperfection and shows it to have significant impact in HES communication system. Tutuncuoglu *et al.* [17] and Devillers and Gündüz [21] consider non-ideal behavior of batteries with a threshold-based charging/discharging strategy, but their research effort focuses on cellular network throughput optimization instead of energy saving.

The other key challenge of RE-powered communication systems design is how to efficiently utilize given channel side information (CSI) and energy side information (ESI). In conventional communication systems, BS power consumption is minimized thorough optimizing energy efficiency (as measured in bits/J) with given CSI. In [6], BS power consumption in multi-user OFDMA systems is proposed as a function of the transmission power, the signal processing power and the fixed circuit power to optimize system energy efficiency, which is ratio of the achieved sum throughput and the energy consumed. However, in RE-powered systems, ESI should be also considered, especially when the charge and discharge behavior of batteries is non-ideal. Markov decision processes (MDP) are widely applied to relevant online optimization problems with statistical knowledge of CSI and ESI [22]. However, MDP suffers from the curse of dimensionality with exponential dimension of system states. Lyapunov optimization technique, which has advantages such as low-complexity, computable theoretical bounds and little requirement of prior statistical knowledge, was first applied in RE-powered communication systems in [23]. Lyapunov optimization framework is applied to solve subcarrier power allocation in [24] and user association problem in [16] to minimize power consumption given CSI and ESI as stochastic processes. However, they do not consider the non-ideal battery behavior which will significantly affect the dynamic of batteries and the resulting optimal solution. Wang *et al.* [25] maximize the network utility in multi-hop wireless networks with imperfect batteries and limited RE. The above works do not consider utilizing the data storage of UEs and adapting the transmission accordingly, which will further enhance the energy and QoS performance.

In this work, we focus on mobile video, which is estimated to contribute to over two-thirds of mobile data traffic by 2018 [26]. Hence it is critical to reduce the BS energy consumption while satisfying the QoS requirements of users during video download/streaming. Techniques which adapt streaming quality like dynamic adaptive streaming over HTTP (DASH) [27] have been studied and applied to shape the download traffic. Most previous work addressing energy consumption during video download/streaming [28], [29] focuses on power saving of mobile devices by shaping the traffic transmitted to users and extending the periods of no transmission or idle periods of mobile devices, but do not address reducing BS energy consumption during video download. Abou-Zeid *et al.* [30] propose to schedule transmission given the channel state predictions for wireless video download and adapt the video bitrate to minimize BS energy consumption while the use of RE and UE buffer is not considered. Kwasinski and Kwasinski [31] propose to adapt compression ratio of video traffic to the amount of harvested RE. However, the technique requires perfect distribution information of harvested RE and traffic demand of UEs.

B. *Contributions*

To the best of our knowledge, this is the first work utilizing both energy storage at the BS and data storage at the UEs to minimize grid power consumption of BS and maximize QoS of users in a RE-aware manner. By integrating Lyapunov optimization techniques in [23] and [32], the original stochastic optimization problem is transformed to a series of operations determined by solving the per-time slot problem which only requires instantaneous information of harvested RE and channel condition. We then develop an online control scheme to solve the per-time slot problem, which consists of: a) charging/discharging algorithm based on current battery level, b) BS subcarrier allocation based on channel condition and buffer level of UEs and battery level

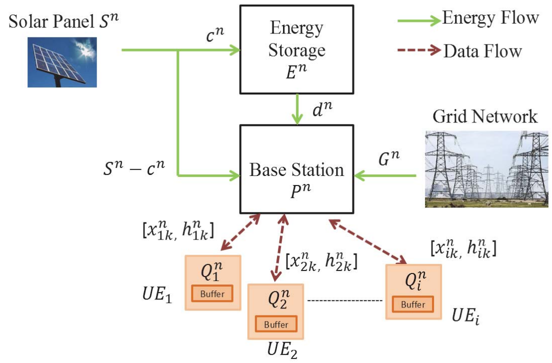

Fig. 1. Architecture of proposed system.

and c) buffer consumption rate based on current buffer level of UEs and QoS requirement. We derive a rigorous analysis to demonstrate that the proposed scheme is feasible for any given finite battery and buffer capacities and the proposed scheme can achieve asymptotically to the optimal solution. The rest of the paper is organized as follows. In Section II, the system model is described and the problem formulation is presented. We present the proposed Lyapunov-based solar power-aware BS resource (L-SPAR) allocation methodology and algorithm in Section III. In Section IV, the feasibility and performance bounds are derived. The performance of the proposed algorithm is evaluated via simulation in Section V. Finally, we conclude the paper in Section VI.

II. System Model and Problem Formulation

In this section, we will first present the system model comprising of network, channel, traffic demand, BS energy consumption, energy storage and data buffer models. Then, we formulate the weighted sum optimization problem to address both grid energy consumption and QoS of users with constraints of UE data buffer, energy storage and BS utilization. For ease of reference, we list the key notations of our system model in Table I.

A. Network and Channel Model

Consider downlink communication in a OFDMA cellular network system with a set of BSs $\boldsymbol{B}$, each with subcarriers set $\boldsymbol{K} = \{1, 2 \ldots K\}$. Without loss of generality, we will consider one BS, $b \in \boldsymbol{B}$ and its associated set of users $\boldsymbol{I} = \{1, 2 \ldots I\}$. For the sake of notational brevity, henceforth, we will drop the subscript b from the BS related variables. Also, we will use the terms energy storage and battery interchangeably. Fig. 1 shows a single BS, with energy flows from different energy sources (PV panel, grid and battery), to different energy sinks (the BS and the battery), and data links between the BS and $\boldsymbol{I}$ users. Transmission time is equally divided into n time slots of duration λ, which is normalized to one in our paper for ease of analysis. We assume perfect channel state estimation including path loss, multi-path fading, shadowing and other factors if any at both the transmitters (BSs) and the receivers (UEs). Each subcarrier $k \in \boldsymbol{K}$ can only be used by one user and subcarrier allocation is performed at the beginning of each time slot. We denote subcarrier allocation by the binary matrix $\boldsymbol{X}^n = \{x_{ik}^n\}_{i \in \boldsymbol{I}, k \in \boldsymbol{K}}$ where x_{ik}^n is defined as

$$x_{ik}^n = \begin{cases} 1, & \text{if subcarrier } k \text{ is assigned to user } i \text{ in n}^{th} \text{ slot} \\ 0, & \text{otherwise} \end{cases} \tag{1}$$

TABLE I
Summary of Key Notations

Notation	Description
$\boldsymbol{K}$	Index set of subcarriers of BS b
$\boldsymbol{I}$	Index set of the UEs associated with b
x_{ik}^n	Subcarrier allocation indicator in n^{th} slot
h_{ik}^n	Channel gain of user i on subcarrier k
r_{ik}^n	Achievable transmission rate of user i on subcarrier k
R_i^n	Total achievable transmission rate of user i
Q_i^n	Buffer level of user i
δ_i^n	Buffer consumption rate of user i
$U_i(\delta)$	Utility function of user i
P^n	Power consumption of the BS in n^{th} slot
E^n	Battery level in n^{th} slot
c^n	Charging energy in n^{th} slot
d^n	Discharging energy in n^{th} slot
θ_0	Perturbation parameter of battery level
θ_i	Perturbation parameter of buffer level of user i

Let $\boldsymbol{H}^n = \{h_{ik}^n\}_{i \in \boldsymbol{I}, k \in \boldsymbol{K}}$ be the channel gain matrix where h_{ik}^n is the channel gain of user i on subcarrier k. The channel gain h_{ik}^n of each BS-UE link is assumed to be statistically independent and identically distributed (i.i.d) and remains constant during each slot. We denote P_k^n the downlink transmit power allocated on each subcarrier k of the BS in the n^{th} slot and is assumed to be fixed within each time slot. Since joint optimization of subcarrier and power allocation is proved to be NP-hard [33] and there is no standard method for optimal solution, our proposed technique only decides subcarrier allocation $\boldsymbol{X}^n$ and it can work with any existing power allocation techniques. Let r_{ik}^n denote the achievable transmission rate from the BS to user i on subcarrier k in the n^{th} slot and is given by

$$r_{ik}^n = W \log_2\left(1 + \frac{\left|h_{ik}^n\right|^2 P_k^n}{\sigma N_0}\right) \tag{2}$$

where W, N_0 and σ are the bandwidth of each subcarrier, noise power density and the nominal spectral efficiency in (bit/s)/Hz respectively. Note that r_{ik}^n is clipped within $[r^{min}, r^{max}]$ to account for practical modulation orders. Let R_i^n denote the total achievable transmission rate from the BS to user i over all subcarriers and is given by

$$R_i^n = \sum_{k=1}^{K} x_{ik}^n r_{ik}^n. \tag{3}$$

B. UE QoS Model

As discussed earlier, we focus on mobile video download/streaming. Video contents can be transmitted to UEs and stored at the UEs' buffer, and then the transmission can be paused without stalling if there is enough data for playing. Therefore, we are interested in the data buffer level of the users. We define the buffer level Q_i^n of user *i* in n^{th} slot as the sum of the buffer level in $n-1^{th}$ slot and the data accumulated in the buffer λR_i^n subtracted by the data used for video playback $\lambda \delta_i^n$. Note that λ is assumed to be 1 in our case. Therefore, buffer level in the n^{th} slot Q_i^n is given by

$$Q_i^{n+1} = Q_i^n + R_i^n - \delta_i^n, \quad \forall i, \quad \forall n, \tag{4}$$

We assume $Q_i^0 = 0, \forall i$ and δ_i^n is the buffer consumption rate satisfying

$$0 \le \delta_i^n \le \delta^{max} \tag{5}$$

with a finite δ^{max} at all time. For smooth playback δ_i^n and R_i^n should be decided in a manner that the video buffer does not overflow or underflow. Hence for each user we have

$$0 \le Q_i^n \le Q_i^{max}, \quad \forall i, \quad \forall n, \tag{6}$$

where $Q_i^{max} \in (0, \infty)$ is the maximum number of bits that can be stored at user *i*, which may depend on the video client and network policy. In DASH [24], the video content is segmented into small HTTP-based files. Video segments are then pre-encoded in multiple versions with their "quality levels," specifying specific video bit rate and resolution [27], [34]. During video download, the streaming adaptation engine at UE *i* selects the quality level of requested video segments based on throughput estimation and media playout conditions [34]. The better QoS UEs have, the higher the buffer consumption rate. To provide a measure of user QoS during video download, we denote utility function[1] $U_i(\delta_i^n)$ for each user *i*. Every $U_i(\delta)$ is assumed to be positive, increasing, strictly concave and differentiable for $\delta \in [0, \delta^{max}]$ [25], [35]. For convenience, we denote β_i as the maximum first derivative of $U_i(\delta)$ according to the property of strictly concave functions.

C. Base Station Power Consumption Model

According to [5], [6], and [11], the BS power consumption can be modeled as a constant power term plus a radio frequency (RF) related power term. Secondly, the RF related power term can be modeled as a linear function of the number of active subcarriers. The total power consumption of the BS in time slot *n* is:

$$P^n = \sum_{i=1}^{I} \sum_{k=1}^{K} x_{ik}^n \left(\frac{P_{tx}}{\Delta} + P_{sp} \right) + P_0 \tag{7}$$

where P_{tx} is the constant transmit power level per subcarrier and Δ is power amplifier efficiency. P_{sp} denotes the signal processing power per subcarrier and P_0 denotes fixed circuit power consumption of the BS such as the baseband processor, the converter and the cooling system. Finally, the energy consumption of the BS in time slot *n* is λP^n and again λ is omitted since λ is assumed to be 1 in our case.

[1]Network utility function is first proposed by Kelly *et al.* [35] as a measure of user satisfaction based on data rate. Increasing, differentiable, and concave utility functions $U(\cdot)$ (e.g., proportional-fair utility functions) are widely adopted in network utility maximization (NUM) problems.

D. Energy Storage

Let the amount of harvested solar at the beginning of the n^{th} slot be S^n. We assume that S^n is immediately available for use in n^{th} slot and takes values in some finite set $S^n \in [0, S^{max}]$ and there exists $S^{max} < \infty$. We also assume that S^n is i.i.d. among different time slots. Although the i.i.d. process cannot fully represent the non-linear and non-stationary solar arrival, it captures the intermittent nature of solar and has been widely adopted in previous studies [16], [22], [23]. The BS stores the harvested solar in the battery and let $E^{max} \in (0, \infty)$ denote the battery capacity. At the beginning of the n^{th} time slot, the transmitter harvests and stores the c^n units of energy. It then draws d^n units of energy from the battery to power the BS. We assume $E^0 = 0$ and model the battery level E^n as

$$E^{n+1} = \varphi E^n + \eta c^n - d^n, \quad \forall n, \tag{8}$$

where c^n and d^n are two non-negative numbers denoting the amount of energy used to charge and discharge the battery in the n^{th} slot respectively. To characterize the imperfection of batteries, we firstly use $\varphi \in (0, 1)$ as storage efficiency. This implies that during each time slot, $(1-\varphi)$ portion of the energy stored in the battery will be lost due to energy dissipation. We use $\eta \in (0, 1)$ to denote the charging efficiency of the battery. When c^n units of energy are used for charging, only ηc^n can be stored in the battery for future use and $(1-\eta)c^n$ is lost due to charging loss.[2]

We assume that $E^0 = 0$ and E^n is constrained by energy causality and limited capacity of the battery. Hence, E^n should satisfy

$$0 \le E^n \le E^{max}, \quad \forall n. \tag{9}$$

As shown in Fig. 1, the grid energy consumption G^n in the n^{th} slot is given by the BS energy consumption P^n subtracted the energy drawn from the battery d^n and the portion of solar energy $S^n - c^n$

$$G^n = P^n - d^n - S^n + c^n \ge 0, \quad \forall n. \tag{10}$$

Note that G^n can never be negative, i.e., there is no transfer of energy back to the grid from the BS for general power grids. c^n is constrained by

$$0 \le c^n \le S^n, \quad \forall n, \tag{11}$$

Therefore, d^n is constrained by

$$0 \le d^n \le P^n, \quad \forall n. \tag{12}$$

E. Problem Formulation

To minimize grid energy consumption while maximizing the utility of users, the weighted sum of the above two objectives is used as our objective. Given the solar energy S^n and the channel conditions $\boldsymbol{H}^n$, the buffer availability of each user Q_i^n

[2]Practically, energy loss occurs during both charge and discharge, and the efficiency depends on factors such as temperature, charging/discharging rate and battery level. For simplicity, these two losses are combined into one and the efficiency is assumed fixed in this work.

and the battery level E^n, our objective is to determine subcarriers allocation $\boldsymbol{X^n}$, the buffer consumption rate δ_i^n, charging energy c^n and discharging energy d^n in each time slot to optimize the objective function while satisfying the buffer constraints of users, the battery constraint and the BS utilization constraint. Therefore, the optimization problem **P1** can be formulated as

$$\textbf{P1:} \min_{X^n,\delta_i^n,c^n,d^n} \lim_{N\to+\infty} \frac{1}{N}\sum_{n=0}^{N-1}\mathbb{E}\left[w_G G^n - w_I\sum_{i=1}^{I} U_i(\delta_i^n)\right]$$

$$s.t.\ (5),(6),(9)-(12) \tag{13}$$

$$\sum_{i=1}^{I} x_{ik}^n \le 1, \quad \forall i, \quad \forall n, \quad \forall k, \tag{14}$$

Constraints (14) states that each subcarrier is exclusively assigned to a single user. Note that since our objective is to maximize aggregate utility of users, we will take negative terms for all $U_i(\delta_i^n)$ in the objective function. Letw_G and w_I denote the weights of the grid energy consumption and aggregate user utility respectively. By properly adjusting w_G and w_I, solving **P1** can effectively minimize grid power consumption with any QoS requirement, depending on the network policy.

The problem **P1** is a stochastic optimization problem. As shown in (6) and (9), the feasible actions set (charging, discharging, the buffer consumption rate and BS resource allocation) is confined by the current UE buffer level and the battery level. Also, the state transition can be described as a function of actions $\{\boldsymbol{X^n}, \delta_i^n, c^n, d^n\}$ and their states $\{E^n, Q_i^n\}$ in the previous time slot given the probability distribution of the solar energy S^n and the channel conditions $\boldsymbol{H^n}$. Such problems can be modeled by MDP and theoretically solved by linear programming (LP) or dynamic programming (DP) techniques [13], [17]. However, the performance of such techniques depends on accurate statistical estimation of solar arrival and channel condition. Furthermore, the offline solution provided by MDP requires exponential number of states to characterize the system, so the process is practically infeasible due to computation complexity. For example, if we have *J* states of solar arrival, *M* states of channel gain and *L* states of buffer level for each user *i* and *T* states of battery levels, we need to solve the MDP problem with JM^iL^iT possible states.

Inspired by Lyapunov optimization framework developed in recent works [23], [32], we will next present a low-complexity online L-SPAR algorithm with the following advantages:

- The proposed algorithm provides an online solution requiring no prior knowledge of the probability distribution of the wireless channel or solar arrival processes.
- The proposed algorithm minimizes objective function considering only the current data buffer and the energy storage state, which greatly reduces the complexity that standard MDP/LP solutions would have faced to solve **P1**.
- Although the proposed algorithm does not result in exact optimal solution, the performance can achieve arbitrarily close to the optimal solution by adjusting the penalty parameter [23] in the Lyapunov optimization framework which will be discussed in Section IV.

III. L-SPAR Methodology and Algorithm

In this section, we will first describe the proposed Lyapunov optimization framework and propose a per-time slot problem **P2**. To solve **P2**, we then propose an online algorithm which determines the BS subcarrier allocation, the amount of energy charging/discharging the battery, and buffer consumption rate of users. In Section IV, we will show that the proposed algorithm provides a feasible and asymptotically optimal solution for **P1**.

A. Per-Time Slot Problem and L-SPAR Algorithm

In constraints (6) and (9), there exists time-dependent coupling between the state of battery and data buffer and the decision of charging/discharging, BS resource allocation and buffer consumption rate across time slots, which makes the optimization challenging. The principle we apply Lyapunov optimization here is to decouple such dependency by transforming such constraints of the battery level E^n and the data buffer level Q_i^n into a set of virtual queues. Based on Lyapunov optimization framework, the objective function in **P1** is defined as penalty function. By greedily minimizing a weighted function of Lyapunov drift, which is the sum of the squares of the current queue backlogs, and the penalty function, the objective function can be optimized with the long-term average constraints satisfied. Traditional Lyapunov optimization can only guarantee to satisfy long-term averaged constraints. To ensure deterministic bounds on all queue sizes derived from (6) and (9), we use the similar method as in [32] to introduce perturbation parameter $\boldsymbol{\theta} = \{\theta_{0,}\theta_1, \dots \theta_I\}$ and define the virtual queues, which represent the shifted version of original battery level E^n and data buffer level Q_i^n. The physical meaning of $\boldsymbol{\theta}$ is the convergence value of data and batteries buffer and was chosen carefully to satisfy the original queue constraints

$$\tilde{E}^n = E^n - \theta_0, \tag{15}$$

$$\tilde{Q}_i^n = Q_i^n - \theta_i, i = 1, 2, \dots, I, \tag{16}$$

where

$$w_G V + \frac{P^{\max}}{\varphi} \le \theta_0 \le \frac{w_G V}{\eta} + \frac{E^{\max} - S^{\max}}{\varphi}, \tag{17}$$

$$w_I V \beta_i + \delta^{\max} \le \theta_i, i = 1, 2, \dots, I, \tag{18}$$

where V denotes the non-negative weight parameter in Lyapunov optimization where larger *V* will place more emphasis on penalty minimization over the queue stability. Note that although the battery and the data buffer levels are always non-negative according to constraints (6) and (9), the virtual queues $\tilde{E}^n$ and $\tilde{Q}_i^n$ can be negative.

We now define the per-time slot problem **P2**, which minimizes the weighted sum of the drift of virtual queues and the penalty function with all constraints except (6) and (9). We will later show that (6) and (9) are indeed satisfied by

Algorithm 1 L-SPAR Algorithm

Initialization: Choose a pair of $(\boldsymbol{\theta}, V)$ which satisfies (17)-(18).

At the beginning of each time slot n, obtain solar energy S^n, virtual battery level queue $\tilde{E}^n$, channel gain $\boldsymbol{H}^n$ and virtual buffer level queue $\tilde{Q}_i^n\ \forall i \in \mathbf{I}$.

Decide optimal action set $\{\boldsymbol{X}^{n*}, \delta_i^n, c^{n*}, d^{n*}\}$ by solving **P2**

Update $\tilde{E}^n$ and $\tilde{Q}_i^n$ according to (4), (8), (15), (16)

Set $n = n + 1$

L-SPAR in Section IV.

$$\textbf{P2:}\ \min_{\boldsymbol{X}^n, \delta_i^n, c^n, d^n} \sum_{i=1}^{I} \tilde{Q}_i^n \left(\sum_{k=1}^{K} x_{ik}^n r_{ik}^n - \delta_i^n \right) + \tilde{E}^n \Big[\eta c^n - d^n - \Big(\tilde{E}^n + \theta_0 \Big)(1-\varphi) \Big] + V \Bigg[w_G (P^n - S^n + c^n - d^n) - w_I \sum_{i=1}^{I} U(\delta_i^n) \Bigg] \tag{19}$$

$$s.t.\ (5),\ (10)-(12),\ (14)$$

After integrating and generalizing Lyapunov optimization framework to propose **P2**, we present the online L-SPAR algorithm. The objective of L-SPAR is to stabilize the battery and data buffer levels around the perturbed level $\boldsymbol{\theta}$ and meanwhile minimize the penalty function. We assume that I users are scheduled in each time slot and the channel state information and buffer level information of users are periodically reported to the BS using Channel Quality Indicator (CQI) and mechanisms similar to Buffer Status Report (BSR) during uploading as in 3GPP specification [36]. Based on the above information and the amount of generated solar energy and the current battery level, the BS will run L-SPAR in every slot. In other words, given a pair of $(\boldsymbol{\theta}, V)$ and by observing the current state of random processes $\{S^n, \boldsymbol{H}^n\}$ and queues $\{\tilde{E}^n, \tilde{Q}_i^n\}$, L-SPAR will determine an optimal action set $\{\boldsymbol{X}^{n*}, \delta_i^n, c^{n*}, d^{n*}\}$ as a solution for **P2**. In the next section, we will focus on solving the per-time slot problem.

B. Solving the Per-Time Slot Problem

Next, we will focus on solving **P2**. After rearranging **P2** and using Eq. (8), the BS energy consumption model, the objective function in (19) can be written as

$$\min_{\boldsymbol{X}^n, \delta_i^n, c^n, d^n} \sum_{i=1}^{I} \tilde{Q}_i^n \left(\sum_{k=1}^{K} x_{ik}^n r_{ik}^n \right) - \sum_{i=1}^{I} \Big[\tilde{Q}_i^n \delta_i^n + w_I V U(\delta_i^n) \Big] + w_G V \sum_{i=1}^{I} \sum_{k=1}^{K} x_{ik}^n \left(\frac{P_{tx}}{\Delta} + P_{sp} \right) + c^n \Big(\eta \tilde{E}^n + w_G V \Big) - d^n \Big(\tilde{E}^n + w_G V \Big) + C$$

where C represents the constant term $\tilde{E}^n(\tilde{E}^n + \theta_0)(1-\varphi) + w_G V(P_0 - S^n)$ in n^{th} slot, which can be omitted in the optimization process. We will decouple the problem into three parts: 1) Charge and discharge of the battery, 2) BS resource allocation, 3) UE buffer consumption rate.

Charge and discharge of the battery: To decide c^{n*} and d^{n*}, we first solve the problem as a simple threshold-based structure

$$\min_{c^n, d^n} c^n(\eta \tilde{E}^n + w_G V) - d^n \Big(\tilde{E}^n + w_G V \Big) \tag{20}$$

$$s.t.\ (10), (11), (12).$$

Case 1: $\eta \tilde{E}^n + w_G V > 0$; $-(\tilde{E}^n + w_G V) \le 0$. L-SPAR will discharge as much as possible and will not charge. Since d^{n*} has to satisfy $P^n - S^n + c^n - d^n \ge 0$ and $c^{n*} = 0$ in this case, we have $d^{n*} = max\{P^n - S^n, 0\}$.

Case 2: $\eta \tilde{E}^n + w_G V > 0$; $-(\tilde{E}^n + w_G V) > 0$. L-SPAR will neither charge nor discharge in n^{th}slot. Therefore, $c^{n*} = d^{n*} = 0$.

Case 3: $\eta \tilde{E}^n + w_G V \le 0$; $-(\tilde{E}^n + w_G V) > 0$. L-SPAR will charge as much as possible and will not discharge at n^{th} slot. Since c^{n*} has to satisfy constraint (12), we have $c^{n*} = S^n$ and $d^{n*} = 0$.

Case 4: $\eta \tilde{E}^n + w_G V \le 0$; $-(\tilde{E}^n + w_G V) \le 0$. Case 4 will not happen since it contradicts with our assumption $0 < \eta < 1$ and $V > 0$.

Note that if $S^n > P^n + c^n$, in this case, the portion of harvested solar $S^n - P^n - c^n$ can not be utilized either to charge the battery or power the BS and will be wasted. Furthermore, when $-V \ge \tilde{E}^n \ge \frac{-V}{\eta}$, we have $c^{n*} = d^{n*} = 0$, which may lead to a "static zone" where there is no further charge and discharge of the battery. However, there is a $(1-\varphi)$ portion of the energy stored in the battery which will be lost due to leakage, so the battery will not be trapped in the static zone in our algorithm.

BS resource allocation: After solving the charge and discharge problem as a function of P^{n}, we will solve the BS resource allocation $\boldsymbol{X}^n$ based on the three possible cases derived from the charge and discharge decision.

Case 1: We have $c^{n*} = 0$ and $d^{n*} = max\{P^n - S^n, 0\}$. We will first solve $\boldsymbol{X}^n$ assuming $d^{n*} = P^n - S^n$. Rewriting **P2** and omitting the constant terms, we want to solve

$$\min_{\boldsymbol{X}^n} \sum_{i=1}^{I} \tilde{Q}_i^n \left(\sum_{k=1}^{K} x_{ik}^n r_{ik}^n \right) - \tilde{E}^n \sum_{i=1}^{I} \sum_{k=1}^{K} x_{ik}^n \left(\frac{P_{tx}}{\Delta} + P_{sp} \right)$$
$$= \min_{\boldsymbol{X}^n} \sum_{i=1}^{I} \sum_{k=1}^{K} x_{ik}^n \left(\tilde{Q}_i^n r_{ik}^n - \tilde{E}^n \left(\frac{P_{tx}}{\Delta} + P_{sp} \right) \right)$$
$$\overset{(a)}{\Leftrightarrow} \sum_{k=1}^{K} \min_{\boldsymbol{X}^n} \sum_{i=1}^{I} x_{ik}^n \left(\tilde{Q}_i^n r_{ik}^n - \tilde{E}^n \left(\frac{P_{tx}}{\Delta} + P_{sp} \right) \right) \tag{21}$$
$$s.t.\ (14)$$

where (a) is because multiple subcarriers can be allocated to one single user. Therefore, the minimization problem can be viewed as the sum of K minimization problems in each subcarrier.

For simplicity, we define $y_{ik}^n = (\tilde{Q}_i^n r_{ik}^n - \tilde{E}^n(\frac{P_{tx}}{\Delta} + P_{sp}))$. To minimize the per-subcarrier problem, the solution for the optimal BS resource allocation is to select one user with the minimal and negative y_{ik}^n. If all y_{ik}^n are non-negative on subcarrier K, the BS will not allocate subcarrier K to any user. The optimal solution x_{ik}^{n*} is given as

$$x_{ik}^{n*} = \begin{cases} 1, \text{ if } y_{ik}^n \le \min\Big\{0, y_{k,min}^n\Big\} \\ 0, \text{ otherwise} \end{cases} \tag{22}$$

where $y_{k,min}^n = \min\limits_{i \in \boldsymbol{I}, k'=k} y_{ik'}^n, k = 1, 2, \ldots, K$. If the resulting $P^{n*} < S^n$ given x_{ik}^{n*}, there is no feasible solution for $d^{n*} = P^n - S^n$. We can set $d^{n*} = 0$ and solve $\boldsymbol{X}^n$ as the same method in Case 2 where $c^{n*} = d^{n*} = 0$.

Case 2 & 3: We have $c^{n*} = 0$ and $c^{n*} = S^n$ in Case 2 and Case 3 respectively while $d^{n*} = 0$ in both cases. Note that no matter $c^{n*} = 0$ or $c^{n*} = S^n$, the $c^n(\eta \tilde{E}^n + w_G V)$ term in **P2** remains a constant in n^{th} slot which does not affect the decision of $\boldsymbol{X}^n$. After rewriting **P2** and omitting the constant terms, we want to solve

$$\min_{\boldsymbol{X}^n} \sum_{i=1}^{I} \tilde{Q}_i^n \left(\sum_{k=1}^{K} x_{ik}^n r_{ik}^n \right) - w_G V \sum_{i=1}^{I} \sum_{k=1}^{K} x_{ik}^n \left(\frac{P_{tx}}{\Delta} + P_{sp} \right)$$
$$= \min_{\boldsymbol{X}^n} \sum_{i=1}^{I} \sum_{k=1}^{K} x_{ik}^n \left(\tilde{Q}_i^n r_{ik}^n + w_G V \left(\frac{P_{tx}}{\Delta} + P_{sp} \right) \right) \tag{23}$$
$$s.t. \ (14).$$

Similar as Case 1, if we set $y_{ik}^{n'} = (\tilde{Q}_i^n r_{ik}^n + w_G V(\frac{P_{tx}}{\Delta} + P_{sp}))$, we have the optimal solution x_{ik}^{n*} given as

$$x_{ik}^{n*} = \begin{cases} 1, \text{ if } y_{ik}^{n}{}' \le \min\Big\{0, \quad y_{k,min}^{n'}\Big\} \\ 0, \text{ otherwise} \end{cases} \tag{24}$$

where $y_{k,min}^{n'} = \min\limits_{i \in \boldsymbol{I}, k'=k} y_{ik'}^{n'}, k = 1, 2, \ldots, K$. For each subcarrier K in all three cases, the user with minimal $\tilde{Q}_i^n r_{ik}^n$ will be selected as potential candidate to serve. The physical interpretation is that among the users whose data buffer levels are lower than their perturbed levels θ_i, the BS will serve the user with the largest product of achievable transmission rate and the gap to their predefined buffer level θ_i in order to fill the gap. On the other hand, if the buffer levels of all users are larger than θ_i, BS will not allocate subcarriers or serve the user with smallest product of achievable transmission rate and excess data compared to their perturbed buffer level θ_i to avoid buffer overflow. After selecting the potential candidate, the algorithm compares $\tilde{Q}_i^n r_{ik}^n$ with either $\tilde{E}^n(\frac{P_{tx}}{\Delta} + P_{sp})$ or $-w_G V(\frac{P_{tx}}{\Delta} + P_{sp})$, depending on whether the BS is powered by the battery in Case 1 or grid in Case 2 & 3 respectively. We can observe that if $\tilde{E}^n$ is larger (the battery level is higher) in Case 1 or V is smaller (L-SPAR focuses more on stability of queues over performance) in Case 2 & 3, the BS is more likely to allocate subcarriers to users and hence consumes more energy.

UE buffer consumption rate: To obtain the optimal UE buffer consumption rate δ_i^n, we solve the problem

$$\min_{\delta_i^n} - \sum_{i=1}^{I} \Big[\tilde{Q}_i^n \delta_i^n + w_I V U(\delta_i^n) \Big] \tag{25}$$
$$s.t. \ (5).$$

As we prove below, the optimal solution δ_i^{n*} is given as

$$\delta_i^{n*} = \min\{\delta^{\max}, U_i'^{-1}\left(\frac{-\tilde{Q}_i^n}{w_I V} \right)\} \tag{26}$$

where $U_i'^{-1}(\cdot)$ is the inverse function of $U_i'(\delta)$ and satisfies $U_i'^{-1}(U_i'(\delta)) = \delta$ for $\delta \in [0, \delta^{\max}]$.

Proof: The minimization problem can be viewed as the sum of I minimization problems for each user. The objective function for each user is a strictly convex function for $\delta \in [0, \delta^{\max}]$ since it is the negative sum of a linear function and a strictly concave function $U_i(\delta)$. Moreover, if the derivative of a strictly convex function is zero at some point which is $\delta_i^n = U_i'^{-1}(\frac{-\tilde{Q}_i^n}{w_I V})$ in our case, then that point is a global minimum. For $\tilde{Q}_i^n \le -w_I V U_i'(\delta^{\max})$, the optimal point $\delta_i^n = U_i'^{-1}(\frac{-\tilde{Q}_i^n}{w_I V})$ is within $[0, \delta^{\max}]$. For $\tilde{Q}_i^n > -w_I V U_i'(\delta^{\max})$, $U_i'^{-1}(\frac{-\tilde{Q}_i^n}{w_I V})$ is not within $[0, \delta^{\max}]$ and hence not a feasible solution. Moreover, since $U_i'(\delta)$ is positive and decreasing for $\delta \in [0, \delta^{\max}]$, the first derivative of objective function $-\tilde{Q}_i^n - w_I V U_i'(\delta_i^n)$ is always negative for $\delta \in [0, \delta^{\max}]$. Therefore, the objective is a monotonically decreasing function for $\delta \in [0, \delta^{\max}]$ and thereby $\delta^{\max}$ is the optimal solution. ∎

In each time slot, the computational complexity of the L-SPAR algorithm comes from the BS resource allocation where sorting y_{ik}^n or $y_{ik}^{n'}$ of I users on each subcarrier requires $O(I \log I)$ time. The complexity of BS resource allocation is then bounded by $O(KI \log I)$ where K is the numbers of subcarriers. As we described in the previous section, the complexity is independent of the complexity of system states (e.g., harvested solar energy, channel state, battery state, UE buffer state) and the choice of $(V, \boldsymbol{\theta})$.

IV. Performance Analysis

In this section, we will show that the L-SPAR algorithm satisfies all constraints in **P1** and provides a theoretical performance bound of L-SPAR. Furthermore, we will discuss the relation between the performance and the choice of the predefined parameters $(V, \boldsymbol{\theta})$ in L-SPAR.

A. Feasibility Analysis

In the proposed L-SPAR algorithm, the UE data buffer constraint (6) and the battery capacity and energy causality constraint (9) are ignored. It is important to show that for given pair of $(V, \boldsymbol{\theta})$, solving the per-time slot problem **P2** will produce feasible solutions of **P1** under the constraints (6) and (9).

Proposition 1: Under the L-SPAR algorithm, the battery level E^n is confined within $[0, E^{\max}]$.

Proof: We first prove E^n is lower bounded by 0. Firstly, we have $E^0 = 0$ from assumption. From L-SPAR we know that $d^{n*} = 0$ when $\tilde{E}^n = E^n - \theta_0 \le -w_G V$. Suppose $0 \le E^n \le \theta_0 - w_G V$, we have $E^{n+1} = \varphi E^n + \eta c^n \ge 0$. On the other hand, if $E^n > \theta_0 - w_G V$, $E^{n+1} \ge \varphi E^n - S^n + P^n \ge \varphi E^n - P^{\max}$. Since $\theta_0 \ge w_G V + \frac{P^{\max}}{\varphi}$ by constraint (17), $E^{n+1} > \varphi(w_G V + \frac{P^{\max}}{\varphi} - w_G V) - p^{max} \ge 0$.

Next, we will show that E^n is upper bounded by $E^{\max}$. Suppose $\frac{-w_G V}{\eta} + \theta_0 \le E^n \le E^{\max}$, from L-SPAR we know the optimal $c^{n*} = 0$. Therefore, $E^{n+1} = \varphi E^n - d^{n*} \le E^n \le E^{\max}$. Otherwise, if $E^n < \frac{-w_G V}{\eta} + \theta_0$, $E^{n+1} \le \varphi E^n + S^{\max} < \varphi\Big(\frac{-w_G V}{\eta} + \theta_0\Big) + S^{\max}$. Since $\theta_0 \le \frac{w_G V}{\eta} + \frac{E^{\max} - S^{\max}}{\varphi}$ by constraint (17), $E^{n+1} \le E^{max}$. ■

Proposition 2: Under the L-SPAR algorithm, the buffer level Q_i^n of user *i* is confined within $[0, Q_i^{max}]$.

Proof: We first prove Q_i^n is lower bounded by 0. If $Q_i^n \ge \delta^{\max}$, $Q_i^{n+1} \ge Q_i^n - \delta \ge 0$ for any $\delta \in [0, \delta^{\max}]$. If $0 \le Q_i^n < \delta^{\max}$, we have $\tilde{Q}_i^n \le \delta^{\max} - \theta_i \le -w_I V U_i{}'(\delta^{\max})$ from (18). Therefore, we have $\delta_i^{n*} = U_i^{'-1}(\frac{-\tilde{Q}_i^n}{w_I V})$ according to (26).

Lemma 1: Given $(V, \boldsymbol{\theta})$ satisfying (17) and (18), we have $U_i{}'(Q_i^n) \le U_i{}'(U_i^{'-1}(\frac{-\tilde{Q}_i^n}{w_I V})), Q_i^n \in [0, \delta^{max}]$

Proof: See Appendix A. ■

Since $U_i(\delta)$ is concave and differentiable for $\delta \in [0, \delta^{\max}]$, $Q_i^{n+1} \ge Q_i^n - \delta_i^{n*} \ge Q_i^n - U_i^{'-1}(\frac{-\tilde{Q}_i^n}{w_I V}) \ge 0$ if and only if $U_i{}'(Q_i^n) \le U_i{}'(U_i^{'-1}(\frac{-\tilde{Q}_i^n}{w_I V}))$, which is derived in Lemma 1. Therefore, with the assumption that $Q_i^0 = 0, \forall i$, we can prove that $Q_i^n \ge 0$.

Next, we will show that Q_i^n is upper bounded by Q_i^{max}.

Lemma 2: $Q_i^n \le \theta_i + \frac{\mu}{r^*}(\frac{P_{tx}}{\Delta} + P_{sp}) + Kr^*$, where $r^* = \max_r \frac{\mu}{r}(\frac{P_{tx}}{\Delta} + P_{sp}) + Kr$, $\mu = \max\{E^{\max} - \theta_0, -w_G V\}$, $r \in [r^{min}, r^{max}]$

Proof: See Appendix B. ■

According to Lemma 2, given the size of the available data buffer Q_i^{max}, we derive the upper bound of the control parameter θ_i

$$\theta_i \le Q_i^{max} - \frac{\mu}{r^*}(\frac{P_{tx}}{\Delta} + P_{sp}) - Kr^* \forall i \tag{27}$$

where constraint $Q_i^n \le Q_i^{max}$ can be satisfied.

The above two propositions together imply that the proposed per-timeslot L-SPAR algorithm with proper selection of $(V, \boldsymbol{\theta})$ can always yield a feasible control policy satisfying constraints (6) and (9) under any arbitrary stochastic process of solar energy S^n and channel conditions $\boldsymbol{H}^n$.

B. Performance Analysis

We will next show that L-SPAR algorithm yields an asymptotically near-optimal solution. By the definition of the drift-plus-penalty function defined in [23], we define Lyapunov function as the total sum of virtual queues length

$$L(n) = \frac{1}{2}\Bigg[\sum_{i=1}^{I}(\tilde{Q}_i^n)^2 + \Big(\tilde{E}^n\Big)^2\Bigg]. \tag{28}$$

Next, the Lyapunov drift is defined as

$$\Delta(n) = \mathbb{E}[L(n+1) - L(n)]. \tag{29}$$

The Lyapunov drift-plus-penalty function is then defined as

$$\Delta_V(n) = \Delta(n) + V\Bigg\{w_G \mathbb{E}\big[G^n\big] - w_I \sum_{i=1}^{I} \mathbb{E}\big[U_i(\delta_i^n)\big]\Bigg\}. \tag{30}$$

Lemma 3: For arbitrary feasible decision variables $\{\boldsymbol{X}^n, \delta_i^n, c^n, d^n\}$, $\Delta_V(n)$ is upper bounded by

$$\begin{aligned}\Delta_V(n) \le \mathbb{E}\Bigg\{ &\sum_{i=1}^{I} \tilde{Q}_i^n \Bigg(\sum_{k=1}^{K} x_{ik}^n r_{ik}^n - \delta_i^n\Bigg) \\ &+ \tilde{E}^n[\,\eta c^n - d^n - (\tilde{E}^n + \theta_0)(1-\varphi)] \\ &+ V\Bigg[w_G(P^n - S^n + c^n - d^n) \\ &- w_I \sum_{i=1}^{I} U(\delta_i^n)\Bigg]\Bigg\} + C_1 \end{aligned} \tag{31}$$

where the constant term C_1 equals to

$$C_1 = \frac{\max\Big\{(\eta S^{\max})^2, [P^{\max} + (1-\varphi)E^{\max}]^2\Big\}}{2} + I\frac{\max\Big[(R^{\max})^2, (\delta^{\max})^2\Big]}{2}.$$

Proof: After subtracting $\boldsymbol{\theta}$ on both sides of (4) and (8), we have

$$\tilde{Q}_i^{n+1} = \tilde{Q}_i^n + R_i^n - \delta_i^n, \tag{32}$$

$$\tilde{E}^{n+1} = \tilde{E}^n + \eta c^{n-1} - d^{n-1} - \Big(\tilde{E}^n + \theta_0\Big)(1-\varphi). \tag{33}$$

By squaring both sides of (32) and (33), and summing up the equalities, we have

$$\begin{aligned}\Delta(n) &= \frac{1}{2}\Bigg[\sum_{i=1}^{I}\Big(\tilde{Q}_i^{n+1}\Big)^2 + \Big(\tilde{E}^{n+1}\Big)^2\Bigg] \\ &\quad - \frac{1}{2}\Bigg[\sum_{i=1}^{I}\Big(\tilde{Q}_i^{n}\Big)^2 + \Big(\tilde{E}^{n}\Big)^2\Bigg] \\ &= \frac{1}{2}\sum_{i=1}^{I}\Bigg(\sum_{k=1}^{K} x_{ik}^n r_{ik}^n - \delta_i^n\Bigg)^2 \\ &\quad + \frac{1}{2}\Big[\eta c^n - d^n - \Big(\tilde{E}^n + \theta_0\Big)(1-\varphi)\Big]^2 \\ &\quad + \sum_{i=1}^{I} \tilde{Q}_i^n \Bigg(\sum_{k=1}^{K} x_{ik}^n r_{ik}^n - \delta_I\Bigg) \\ &\quad + \tilde{E}^n\Big[\eta c^n - d^n - \Big(\tilde{E}^n + \theta_0\Big)(1-\varphi)\Big] \\ &\le \sum_{i=1}^{I} \tilde{Q}_i^n \Bigg(\sum_{k=1}^{K} x_{ik}^n r_{ik}^n - \delta_i\Bigg) \\ &\quad + \tilde{E}^n\Big[\eta c^n - d^n - \Big(\tilde{E}^n + \theta_0\Big)(1-\varphi)\Big] + C_1. \end{aligned}$$

The inequality holds since $x_{ik}^n r_{ik}^n, \delta_i^n, \eta c^n$ and $d^n + (\tilde{E}^n + \theta_0)(1-\varphi)$ are all non-negative. We then add the penalty function $V[w_G(P^n - S^n + c^n - d^n) - w_I \sum_{i=1}^{I} U(\delta_i^n)]$ and take expectation on both sides to obtain the desired result. ■

We then define an auxiliary problem **P3**. In **P3**, the constraints (6) and (9) are replaced by the corresponding time-average version (36) and (37).

$$\textbf{P3:} \quad \min_{X^n, \delta_i^n, c^n, d^n} \lim_{N \to +\infty} \frac{1}{N} \sum_{n=0}^{N-1} \mathbb{E}\left[w_G G^n - w_I \sum_{i=1}^{I} U_i(\delta_i^n) \right]$$

$$s.t. \ (5), (11) - (13), \tag{34}$$

$$\lim_{N \to +\infty} \frac{1}{N} \sum_{n=0}^{N-1} \mathbb{E}\big[R_i^n - \delta_i^n\big] = 0, \quad \forall i, \tag{35}$$

$$0 \le \lim_{N \to +\infty} \frac{1}{N} \sum_{n=0}^{N-1} \mathbb{E}\big[\eta c^n - d^n\big] \le (1-\varphi) E^{max}, \tag{36}$$

Proposition 4: **P3** is the relaxation of **P1** where any feasible solution in **P1** satisfies (35) and (36).

Proof: By summing up both sides of (4) and (8) for $n = 1, 2, \ldots N$, taking the expectation, divide both sides by N and let N go to infinity, we have

$$\lim_{N \to +\infty} \mathbb{E}\left[\frac{Q_i^N}{N}\right] = \lim_{N \to +\infty} \mathbb{E}\left[\frac{Q_i^0}{N}\right] + \lim_{N \to +\infty} \frac{1}{N} \mathbb{E}[R_i^n - \delta_i^n], \ \forall i, \tag{37}$$

$$\lim_{N \to +\infty} \frac{(1-\varphi)}{N} \sum_{n=1}^{N} \mathbb{E}[E^n] = \lim_{N \to +\infty} \mathbb{E}\left[\frac{E^0}{N}\right] + \lim_{N \to +\infty} \frac{1}{N} \mathbb{E}[\eta c^n - d^n]. \tag{38}$$

Since both $Q_i^N < \infty$ and E^n is bounded within $[0, E^{max}]$, (37) and (38) are satisfied. ■

Let Y^{opt} and $\tilde{Y}^{opt}$ be the optimal value of penalty function of **P1** and **P3** respectively. $Y^{opt} \ge \tilde{Y}^{opt}$ since every feasible solution in **P1** satisfies **P3**.

Lemma 4: For arbitrary $\varepsilon > 0$, there exist a stationary control policy $\mathbf{\Pi} = \{\boldsymbol{X}^{\Pi}, \delta_i^{\Pi}, c^{\Pi}, d^{\Pi}\}$ which observes $\{S^n, \boldsymbol{H}^n\}$ for each slot *n* and independently choose a control action in **P3** and satisfies

$$\mathbb{E}\left[G^{n\Pi} - \sum_{i=1}^{I} U_i\left(\delta_i^{n\Pi}\right)\right] \le \tilde{Y}^{opt} + \varepsilon, \tag{39}$$

$$\left|\mathbb{E}\left[R_i^{n\Pi} - \delta_i^{n\Pi}\right]\right| \le \varepsilon, \quad \forall i, \tag{40}$$

$$(1-\varphi) E^{max} \ge \mathbb{E}\left[\eta c^{n\Pi} - d^{n\Pi}\right] \ge 0. \tag{41}$$

Proof: The proof is similar to [23, Th. 4.5], which is omitted for brevity.

Next, we will derive the worst-case performance of L-SPAR algorithm with the auxiliary problem **P3.**

Theorem 1: The objective function achieved by L-SPAR is upper-bounded by $Y^{opt} + \frac{C_2}{V}$ where C_2 is given by

$$C_2 = (1-\varphi) E^{\max} \max\{\theta_0, (E^{\max} - \theta_0)\} + C_1.$$

Note that Y^{opt} is the optimal value of **P1** under any feasible control algorithm, even if which relies on future knowledge of random process $\{S^n, \boldsymbol{H}^n\}$.

Proof: See Appendix C. ■

According to Theorem 1, the gap between the solution achieved by L-SPAR and the optimal solution Y^{opt} is decided by $\frac{C_2}{V}$, and $C_2 = (1-\varphi) E^{\max} \max\{\theta_0, (E^{\max} - \theta_0)\} + \frac{\max\{(\eta S^{\max})^2, [P^{\max} + (1-\varphi) E^{\max}]^2\}}{2} + I \frac{\max[(R^{\max})^2, (\delta^{\max})^2]}{2}$ is a constant with given system parameters. Therefore, we can make the objective function arbitrarily close to theoretical optimal solution Y^{opt} by letting $V \to \infty$. However, increasing *V* comes with a cost of the increasing convergence level of data buffer $w_I V \beta_i + \delta^{\max}$ and batteries buffer $w_G V + \frac{P^{\max}}{\varphi}$, according to equations (17) and (18). In other word, the decision of *V* is a tradeoff between the performance (in terms of grid power consumption and user utility) and longer convergence time and higher buffer requirement. By setting proper values of (w_G, w_I, V), we can adjust the priority of L-SPAR algorithm to meet with different system requirements.

V. Simulation Framework and Results

In this section, we will discuss the developed simulation framework and results obtained by using the proposed L-SPAR algorithm and compare the results with existing methods during mobile video download.

A. Simulation Framework

We have developed a MATLAB based simulation framework which consists of PV harvesting model, BS power consumption model, and traffic demand model of UEs. The framework allows us to implement different video download techniques and evaluate the grid power consumption for temporally varying harvested solar energy and channel conditions. We will briefly describe the above models and the related simulation parameters, as listed in Table II.

In our simulation study, we assume the harvested solar energy S^n is uniformly distributed between 0 and $S^{max} =$ 200W. To show that L-SPAR does not depend on the assumption on the random processes and holds for non-i.i.d cases, we will also include the actual solar irradiance trace in [1] in performance comparison. We assume imperfect batteries at the BS, with storage efficiency $\varphi = 0.99$, and charging efficiency $\eta = 0.8$ and maximum capacity 300J. The linear power consumption model elaborated in Section II is used with the parameters obtained from [36]. For the network and channel model, we assume the BS has 20 subcarriers with equal bandwidth. The cell radius, transmit power, noise power, system bandwidth and channel gain parameters recommended in Long Term Evolution (LTE) specifications [37], [38] are listed in Table II. We assume users are randomly distributed within a 150-meter radius with the total number of concurrent users $I = 10$. The channel gains at each time slot are exponentially distributed with mean equal to path-loss model given in Table II. Different users download videos of different bitrates with utility function $U_i(\delta) = ln(1 + \delta_i)$, We assume each user has maximum buffer size of 500 MB and maximum buffer consumption rate 10MB/s. For the performance metrics, we assume equal weights of the grid power consumption w_G and aggregate user utility w_I in our simulation.

We compare the proposed technique with two existing relevant techniques, [15] and [24], listed below. For convenience, we will refer to them as Approach 1 [15] and Approach 2 [24] respectively. In Approach 1, which makes greedy decisions

TABLE II
SIMULATION PARAMETERS

Cell radius	150m
Simulation time	1hour
Path-loss(dB)	$140.7 + 36.7\, log_{10}\, R$, R is the distance between user and BS and is in kilometers
Noise power	-105.86dBm
Bandwidth BW	10MHz
Max transmit power	4W
Maximum BS power	140W
Static BS power	35W
Number of users	10
UE Buffer size	500 MB

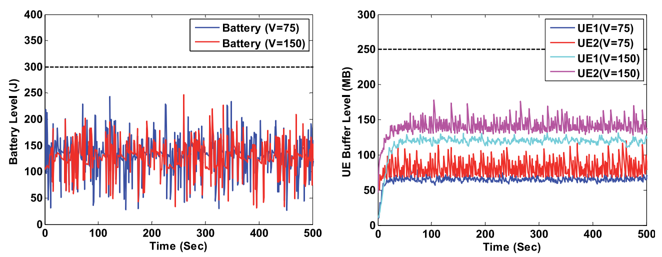

(a) (b)

Fig. 2. (a) left, battery level versus time (b) right, buffer level of two users versus time.

to minimize the objective function, the UEs first choose the largest possible buffer consumption rate considering its available downloaded data. Secondly, Approach 1 arranges the UEs in an ascending order with respect to their remaining data in their buffers. The BS then gives higher priority for using the harvested RE and only allocates the subcarrier with the best channel gain to the UE which buffer level is below a minimal level, which is the maximum buffer consumption rate δ^{max} in our simulation. In other words, the BS only allocates the minimum required resources (determined by the buffer consumption rate and buffer level) to the users while UEs try to maximize their utility. Approach 2 uses standard Lyapunov optimization framework while perfect batteries are assumed. The method is similar to L-SPAR instead of two key differences: 1) instead of using data buffer to halt or reduce data transmission, the BS allocates enough subcarriers to meet the required buffer consumption rate of UEs in each time slot, 2) the optimization process does not consider the effect of battery imperfection.

B. Simulation Results

The simulation results consist of two parts: We will first verify the feasibility of L-SPAR algorithm by examining the battery level of the BS and the UE buffer level. Secondly, we will compare L-SPAR with the other methods using the weighted sum of grid energy consumption and aggregate user utility defined in (13) and the corresponding required battery and UEs' buffer. In our simulation, the value of θ_0 and θ_i are chosen as the LHS of (17) and (18) respectively, which means the minimum value of θ_0 and θ_i are chosen with given V, the non-negative weight parameter in Lyapunov optimization where larger V emphasizes more on objective minimization over the queue stability. The rationale is that the larger the perturbation parameter θ_0 and θ_i, L-SPAR tends to maintain unnecessarily higher battery level and buffer level of UEs. We choose $V = 75$ and $V = 150$ as two examples to discuss how different values of V affect the dynamics of the battery and the UEs' buffer level, as shown in Fig. 2. Note we only show the first 500 seconds of the simulation since both targets converge and stabilize within the first 500 seconds.

In Fig. 2(a), we can observe that the battery level in both cases fluctuates with the maximum charge ηS^{max} and the maximum discharge P^{max} and the variation is within the range between 40J and 250J. The major difference between the two cases is the frequency of charging and discharging in $V = 75$ is higher than $V = 150$. When V increases, the gap between charging and discharging threshold also increases, which makes charging and discharging less likely to occur. This also implies that when V increases, L-SPAR charge/discharge the battery less frequently to avoid charging energy loss. In Fig. 2(b), the buffer of two users with their distance to the BS equals to 100m (UE1) and 50m (UE2) are shown. Firstly, we can see that since the average channel gain of UE2 is better than UE1, the buffer level of UE2 converges faster and the convergence level is higher than UE1. This can be explained in the per-time slot problem that the larger the achievable transmission rate of UE i, the more likely the BS will allocate the subcarriers to UE i. Moreover, when V increases to 150, convergence of the buffer of both UEs to a higher level takes longer time, which is the tradeoff between performance matrix and queue size in Lyapunov optimization framework. As shown in Fig. 2, we can conclude that the proposed L-SPAR algorithm is feasible in terms of battery and data buffer.

In Fig. 3, we compare the performance metric, which is the weighted sum of grid energy consumption and aggregate user utility, between the three methods with different values of V. Note that Approach 1 is independent of V. We can see that the weighted sum is inversely proportional to V, which verifies the asymptotic optimality of Theorem 1. Fig. 3(a) further shows that L-SPAR can produce consistently better performance than the other two methods. For example, when $V = 270$, L-SPAR improves the performance by 57.6% and 38.8% compared with Approach 1 and Approach 2 respectively. In Fig. 3(b) and 3(c), we compare the average grid power consumption and aggregate utility of UEs respectively between L-SPAR and Approach 2 (Approach 1 is omitted since it is independent of V). We can see that power consumption decreases as V increases for both methods while the aggregate utility of UEs decreases. Moreover, L-SPAR consistently consumes less power than Approach 2 with the same buffer consumption rate. As an example, when $V = 270$, L-SPAR consumes 25.5% less average power than Approach 2. As shown in Fig. 3, L-SPAR effectively reduces the energy consumption by 37.7% while the aggregate utility of UEs only decreases by 5.9%. In the scenario with actual solar irradiance trace, we assume the solar module associated with the BS uses typical crystalline solar cells with 15% conversion efficiency,

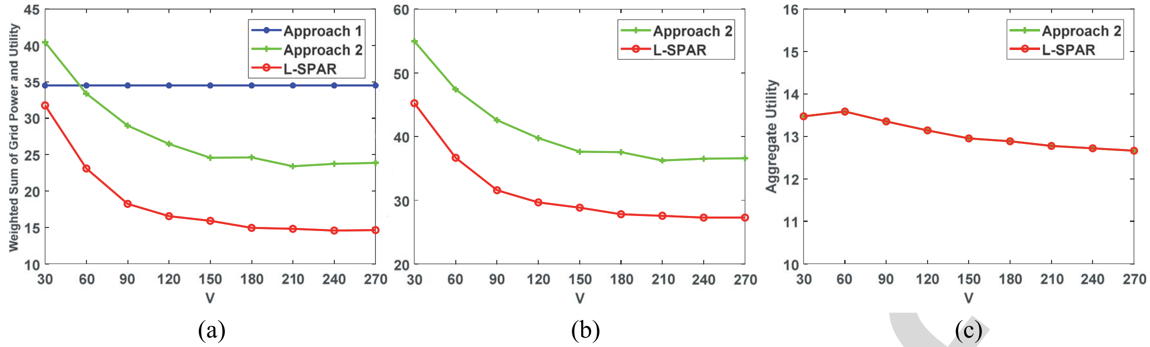

Fig. 3. Performance with uniformly distributed solar trace (a) left, weighted sum of grid power consumption and aggregate user utility vs. V, (b) center, average grid power consumption vs. V and (c) right, aggregate utility of UEs vs. V.

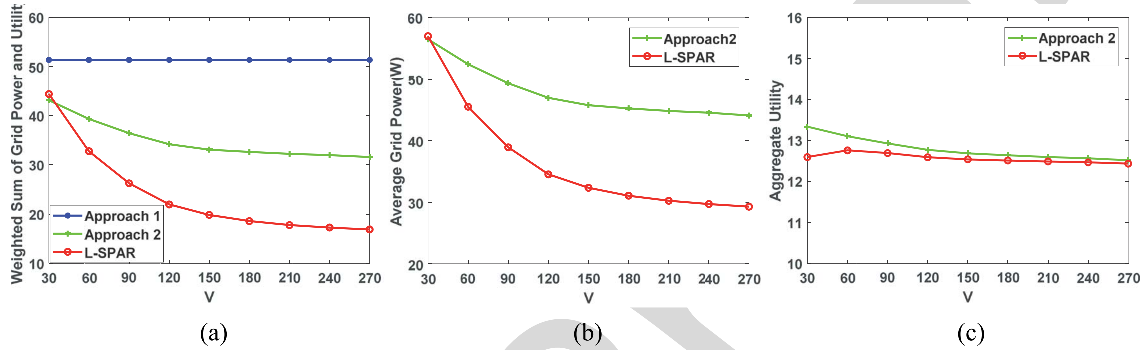

Fig. 4. Performance with actual solar trace (a) left, weighted sum of grid power consumption and aggregate user utility vs. V, (b) center, average grid power consumption vs. V and (c) right, aggregate utility of UEs vs. V.

and measurement of the solar power profile used in [1] for the simulation is from 8AM to 4PM. The performance is generally worse for all three methods because of non-stationary and non-linear solar profile. However, we can observe similar trend as the case with uniformly distributed solar power, as shown in Figure 4. When $V = 270$, L-SPAR improves the performance by 68.1% and 46.8% compared with Approach 1 and Approach 2 respectively.

In Fig. 5, we simulate the maximum battery level and user buffer needed for different values of V. In Fig. 5(a), the maximum battery level in Approach 2 approximately remains the same as V increases while it slightly decreases in L-SPAR. The observation is different from what is discussed in Section IV where the required batter capacity should increase with the increment of θ_0 as V increases. The reason is that the maximum battery level in L-SPAR decreases as V increases is L-SPAR takes charging efficiency into account. In L-SPAR algorithm, L-SPAR will not charge if $\tilde{E}^n \geq \frac{-V}{\eta}$. Applying $\theta_0 = V + \frac{P^{\max}}{\varphi}$ as the setting in our simulation, we have the above threshold as $E^n = \tilde{E}^n + \theta_0 \geq \frac{\eta - 1}{\eta} V + \frac{P^{\max}}{\varphi}$. Since $\frac{\eta-1}{\eta} < 0$, the charging threshold in L-SPAR decrease as V increases, showing that the actual required battery capacity is less than the theoretical bound in (17). In Fig. 5(b), we can observe that the required buffer level of both Approach 2 and L-SPAR is proportional to V. This verifies the performance analysis and the growth of required data buffer of UEs and longer convergence time observed in Fig. 5(b), which becomes the main tradeoff to achieve better grid energy consumption and aggregate user utility.

We will next discuss the effect of choosing different w_G and w_I, the weights associated with grid energy consumption and user utility in equation (13). Grid power consumption and aggregate user utility versus $\frac{w_I}{w_G}$ with $V = 30$ and $V = 270$ are shown in Fig. 6. As $\frac{w_I}{w_G}$ increases, both grid power consumption and user utility increases because the BS tends to consume more power to transmit data to UEs to increase aggregate utility. Secondly, the grid power consumption grows linearly while aggregate utility grows logarithmically with increasing $\frac{w_I}{w_G}$ which indicates the tradeoff between grid power and aggregate utility is not uniform. Thirdly, different values of V result in different tradeoffs between grid power and aggregate utility. For example, from $\frac{w_I}{w_G} = 0.5$ to $\frac{w_I}{w_G} = 1.5$, the ratio of increased aggregate utility to increased grid power is 0.17 when $V = 30$ and 0.20 when $V = 270$, respectively. In conclusion, the parameter set (w_G, w_I, V) in L-SPAR can be chosen to meet the data buffer constraint of UEs and arbitrary priority of grid power consumption and utility of UEs as desired by a specific service provider or network operator.

VI. Conclusion

In this paper, we propose a renewable energy (RE)-aware BS resource allocation technique which aims to better utilize intermittent harvested renewable energy to reduce grid power consumption of hybrid energy supply (HES) BSs and

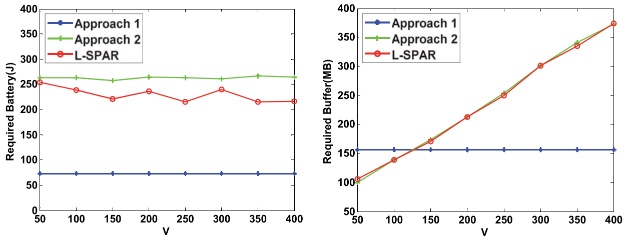

(a) (b)

Fig. 5. (a) left, required battery level vs. V and (b) right, average buffer vs. V.

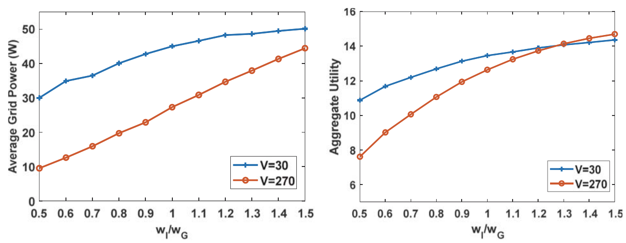

(a) (b)

Fig. 6. (a) left, average grid power consumption vs. $\frac{w_I}{w_G}$ and (b) right, aggregate utility of UEs vs. $\frac{w_I}{w_G}$.

enhance QoS of UEs. We utilize the data buffer of UEs together with energy storage of the BS to adapt the BS resource. Our technique decides optimal charging and discharging of batteries, subcarrier allocation of the BS and buffer consumption rate according to given CSI and ESI. Moreover, a realistic imperfect battery model is considered in our paper.

To avoid the performance degradation due to imperfect prediction of CSI and ESI and reduce the computation complexity, we propose a Lyapunov optimization-based online algorithm in a RE-aware manner. To minimize grid energy consumption while maximizing utility of users, the weighted sum of the above two targets is used as our objective function. To satisfy the causality and capacity constraints of batteries and UEs' buffer, we generalize the Lyapunov optimization technique and propose an online L-SPAR algorithm based on current state of energy arrival, channel condition, battery level and buffer level of UEs. We then prove the feasibility and performance bound of L-SPAR algorithm. The simulation results show that L-SPAR provides a feasible solution and effectively reduces grid power consumption compared to conventional non-RE schemes and existing Lyapunov-based techniques.

Jointly solving power and subcarrier allocation in each time slot can enable full utilization of spatial/temporal diversity of OFDMA networks and can potentially lead to better optimization opportunities and hence better performance. In the future, we plan to explore addressing this more generalized problem, while also addressing its significantly increased complexity. Finally, we plan to extend this research to a cooperative BSs scheme to incorporate both temporal and spatial variation of harvested RE in multi-BSs scenario.

Appendix

A. Proof of Lemma 1

Since $U_i'^{-1}(\cdot)$ is the inverse function of $U_i'(\delta)$ which satisfies $U_i'^{-1}(U_i'(\delta)) = \delta$, we have $U_i'(U_i'^{-1}(\frac{\theta_i-Q_i^n}{w_I V})) = \frac{\theta_i-Q_i^n}{w_I V} \geq \beta_i + \frac{\delta^{\max}-Q_i^n}{w_I V}$ by the definition of (19). Since $\beta_i \geq U_i'(Q_i^n)$ and $\delta^{\max} > Q_i^n$ for $Q_i^n \in [0,\delta^{\max}]$, $U_i'(U_i'^{-1}(\frac{\theta_i-Q_i^n}{w_I V})) \geq U_i'(Q_i^n)$ for $Q_i^n \in [0,\delta^{\max})$.

B. Proof of Lemma 2

Derived from data buffer dynamic equation (4), we have

$$\begin{aligned}\tilde{Q}_i^{n+1} &= \tilde{Q}_i^n + \sum_{k=1}^{K} x_{ik}^n r_{ik}^n - \delta_i^n \\ &\leq \tilde{Q}_i^n + \sum_{k=1}^{K} x_{ik}^n r_{ik}^n, r_{ik}^n \in \left[r^{min}, r^{max}\right].\end{aligned}$$

The inequality comes from (5) that buffer consumption rate δ_i^n is non-negative. From (22) and (24) in L-SPAR, $x_{ik}^n = 1$ only if $\tilde{Q}_i^n r_{ik}^n \leq \tilde{E}^n(\frac{P_{tx}}{\Delta} + P_{sp})$ in Case 1 or $\frac{\mu}{r^{min}}(\frac{P_{tx}}{\Delta} + P_{sp}) < \tilde{Q}_i^n r_{ik}^n \leq -w_G V(\frac{P_{tx}}{\Delta} + P_{sp})$ in Case 2 & 3 respectively. We define $\mu = \max\{E^{\max} - \theta_0, -w_G V\}$. Therefore, we have

$$x_{ik}^n = \begin{cases} 1, & \text{only if } \tilde{Q}_i^n r_{ik}^n \leq \mu(\frac{P_{tx}}{\Delta} + P_{sp}) \\ 0, & \text{otherwise} \end{cases} \tag{42}$$

We then define r^* that $r^* = \max\limits_{r} \frac{\mu}{r}(\frac{P_{tx}}{\Delta} + P_{sp}) + Kr$, $r \in [r^{min}, r^{max}]$. If $\tilde{Q}_i^n \leq \frac{\mu}{r^*}(\frac{P_{tx}}{\Delta} + P_{sp}) + Kr^*$, $\tilde{Q}_i^{n+1} \leq \tilde{Q}_i^n$. On the other hand, if $\tilde{Q}_i^n \leq \frac{\mu}{r^{min}}(\frac{P_{tx}}{\Delta} + P_{sp})$ and together with (42), we have

$$\begin{aligned}\tilde{Q}_i^{n+1} &\leq \max_{i'=i,k\in\boldsymbol{K}} \frac{\mu}{r_{i'k}^n}\left(\frac{P_{tx}}{\Delta} + P_{sp}\right) + Kr_{i'k}^n \\ &\leq \frac{\mu}{r^*}\left(\frac{P_{tx}}{\Delta} + P_{sp}\right) + Kr^* \end{aligned} \tag{43}$$

After adding θ_i on both sides of (43), we can obtain the desired result.

C. Proof of Theorem 1

Together with the upper bound of $\Delta_V(n)$ derived from *Lemma 3* and the property of L-SPAR algorithm, we have

$$\begin{aligned}\Delta_V(n) \leq \mathbb{E}\Bigg\{&\sum_{i=1}^{I} \tilde{Q}_i^n \left(\sum_{k=1}^{K} x_{ik}^{n*} r_{ik}^n - \delta_i^{n*}\right) \\ &+ \tilde{E}^n\left[\eta c^{n*} - d^{n*} - \left(\tilde{E}^n + \theta_0\right)(1-\varphi)\right] \\ &+ V\left[w_G(P^n - S^n + c^{n*} - d^{n*}) - w_I \sum_{i=1}^{I} U(\delta_i^{n*})\right]\Bigg\} \\ &+ C_1 \leq \mathbb{E}\Bigg\{\sum_{i=1}^{I} \tilde{Q}_i^n \left(\sum_{k=1}^{K} x_{ik}^{n\Pi} r_{ik}^n - \delta_i^{n\Pi}\right) \\ &+ \tilde{E}^n\left[\eta c^{n\Pi} - d^{n\Pi} - \left(\tilde{E}^n + \theta_0\right)(1-\varphi)\right] \\ &+ V\left[w_G\left(P^n - S^n + c^{n\Pi} - d^{n\Pi}\right) - w_I \sum_{i=1}^{I} U\left(\delta_i^{n\Pi}\right)\right]\Bigg\}\end{aligned}$$

$$
\begin{aligned}
&+ C_1 = \mathbb{E}\left[\sum_{i=1}^{I} \tilde{Q}_i^n \left(\sum_{k=1}^{K} R_i^{n\Pi} - \delta_i^{n\Pi}\right)\right] \\
&+ \mathbb{E}\left\{\tilde{E}^n \left[\eta c^{n\Pi} - d^{n\Pi} - \left(\tilde{E}^n + \theta_0\right)(1-\varphi)\right]\right\} \\
&+ V\mathbb{E}\left[w_G G^{n\Pi} - w_I \sum_{i=1}^{I} U_i\left(\delta_i^{n\Pi}\right)\right] + C_1 \\
\leq\; & \varepsilon \sum_{i=1}^{I} \max\{(Q_i^{max} - \theta_i, \theta_i\} \\
&+ (1-\varphi)E^{\max}\max\{\theta_0, (E^{\max} - \theta_0)\} \\
&+ V\left(\tilde{Y}^{opt} + \varepsilon\right) + C_1
\end{aligned}
$$

The first inequality is directly obtained from *Lemma 3*. The second inequality is because the solution $\{\boldsymbol{X}^*, \delta_i^*, c^*, d^*\}$ obtained from L-SPAR minimize the per-time slot problem **P2**. Together with the facts in Proposition 1 and 2 that E^n is bounded within $[0, E^{max}]$ and Q_i^n is bounded within $[0, Q_i^{max}]$ respectively, we then apply the performance bound derived from *Lemma 4* to give the last inequality.

From *Lemma 4,* letting $\varepsilon \to 0$ and $C_2 = (1-\varphi)E^{\max}\max\{\theta_0, (E^{\max} - \theta_0)\} + C_1$, we have

$$
\begin{aligned}
\Delta_V(n) &= \mathbb{E}[L(n+1) - L(n)] \\
&\quad + V\left\{w_G \mathbb{E}[G^n] - w_I \sum_{i=1}^{I} \mathbb{E}[U_i(\delta_i^n)]\right\} \\
&\leq V\tilde{Y}^{opt} + C_2. \qquad (44)
\end{aligned}
$$

We then sum up equation (44) for $n = 0, 1, \ldots, N-1$ and divide both sides by N to have

$$
\begin{aligned}
&\frac{1}{N}\{\mathbb{E}[L(N)] - L(0)\} \\
&+ \frac{1}{N}\sum_{n=0}^{N-1} V\left\{\mathbb{E}[G^n] - w_I \sum_{i=1}^{I} \mathbb{E}[U_i(\delta_i^n)]\right\} \\
&\leq V\tilde{Y}^{opt} + C_2 \leq VY^{opt} + C_2
\end{aligned}
$$

Since $\mathbb{E}[L(N)] - L(0) \leq \infty$ from Proposition 1 and 2, by letting $N \to \infty$ and divide both sides by V we have

$$
\lim_{N\to+\infty} \frac{1}{N}\sum_{n=0}^{N-1}\{w_G\mathbb{E}[G^n] - \sum_{i=1}^{I}\mathbb{E}[U_i(\delta_i^n)]\} \leq Y^{opt} + \frac{C_2}{V}.
$$

References

[1] P.-H. Chiang, R. Guruprasad, and S. Dey, "Renewable energy-aware video download in cellular networks," in *Proc. IEEE Symp. Pers. Indoor Mobile Radio Commun. (PIMRC)*, Hong Kong, Sep. 2015, pp. 1622–1627.

[2] *SMARTer2020 Report*, GeSI, Brussels, Belgium, 2013. [Online]. Available: http://gesi.org/SMARTer2020

[3] *Technology Vision 2020: Flatten Network Energy Consumption*, Nokia, Espoo, Finland, 2013. [Online]. Available: http://networks.nokia.com/file/flatten-network-energy-white-paper

[4] D. Feng *et al.*, "A survey of energy-efficient wireless communications," *IEEE Commun. Surveys Tuts.*, vol. 15, no. 1, pp. 167–178, 1st Quart., 2013.

[5] Z. Xu *et al.*, "Energy-efficient configuration of spatial and frequency resources in MIMO-OFDMA systems," *IEEE Trans. Commun.*, vol. 61, no. 2, pp. 564–575, Feb. 2013.

[6] Q. Wu *et al.*, "Resource allocation for joint transmitter and receiver energy efficiency maximization in downlink OFDMA systems," *IEEE Trans. Commun.*, vol. 63, no. 2, pp. 416–430, Feb. 2015.

[7] R. Guruprasad, K. Son, and S. Dey, "Power-efficient base station operation through user QoS-aware adaptive RF chain switching technique," in *Proc. IEEE Int. Conf. Commun. (ICC)*, London, U.K., Jun. 2015, pp. 244–250.

[8] K. Son, H. Kim, Y. Yi, and B. Krishnamachari, "Base station operation and user association mechanisms for energy-delay tradeoffs in green cellular networks," *IEEE J. Sel. Areas Commun.*, vol. 29, no. 8, pp. 1525–1536, Sep. 2011.

[9] M.-L. Ku, W. Li, Y. Chen, and K. J. R. Liu, "Advances in energy harvesting communications: Past, present, and future challenges," *IEEE Commun. Surveys Tuts.*, vol. 18, no. 2, pp. 1384–1412, 2nd Quart., 2016.

[10] Q. Wu, G. Y. Li, W. Chen, D. W. K. Ng, and R. Schober, "An overview of sustainable green 5G networks," *IEEE Wireless Commun.*, vol. 24, no. 4, pp. 72–80, Aug. 2017.

[11] M. Patterson, N. F. Macia, and A. M. Kannan, "Hybrid microgrid model based on solar photovoltaic battery fuel cell system for intermittent load applications," *IEEE Trans. Energy Convers.*, vol. 30, no. 1, pp. 359–366, Mar. 2015.

[12] *Alternative Renewable Power Concepts for Alcatel-Lucent Outdoor Wireless Small Cell Solutions*, Alcatel-Lucent Bell Labs, Murray Hill, NJ, USA, Jan. 2011.

[13] J. Gong, S. Zhou, and Z. Niu, "Optimal power allocation for energy harvesting and power grid coexisting wireless communication systems," *IEEE Trans. Commun.*, vol. 61, no. 7, pp. 3040–3049, Jul. 2013.

[14] X. Huang and N. Ansari, "Energy sharing within EH-enabled wireless communication networks," *IEEE Wireless Commun.*, vol. 22, no. 3, pp. 144–149, Jun. 2015.

[15] T. Zhang, W. Chen, Z. Han, and Z. Cao, "A cross-layer perspective on energy harvesting aided green communications over fading channels," in *Proc. IEEE INFOCOM*, Turin, Italy, 2013, pp. 3230–3235.

[16] Y. Mao, J. Zhang, and K. B. Letaief, "A Lyapunov optimization approach for green cellular networks with hybrid energy supplies," *IEEE J. Sel. Areas Commun.*, vol. 33, no. 12, pp. 2463–2477, Dec. 2015.

[17] K. Tutuncuoglu, A. Yener, and S. Ulukus, "Optimum policies for an energy harvesting transmitter under energy storage losses," *IEEE J. Sel. Areas Commun.*, vol. 33, no. 3, pp. 467–481, Mar. 2015.

[18] M. J. Farooq, H. Ghazzai, A. Kadri, H. ElSawy, and M.-S. Alouini, "A hybrid energy sharing framework for green cellular networks," *IEEE Trans. Commun.*, vol. 65, no. 2, pp. 918–934, Feb. 2017.

[19] M. J. Farooq, H. Ghazzai, A. Kadri, H. ElSawy, and M.-S. Alouini, "Energy sharing framework for microgrid-powered cellular base stations," in *Proc. IEEE GLOBECOM*, Washington, DC, USA, Dec. 2016, pp. 1–7.

[20] X. Huang, T. Han, and N. Ansari, "On green-energy-powered cognitive radio networks," *IEEE Commun. Surveys Tuts.*, vol. 17, no. 2, pp. 827–842, 2nd Quart., 2015.

[21] B. Devillers and D. Gündüz, "A general framework for the optimization of energy harvesting communication systems with battery imperfections," *J. Commun. Netw.*, vol. 14, no. 2, pp. 130–139, Apr. 2012.

[22] J. Yang and S. Ulukus, "Optimal packet scheduling in an energy harvesting communication system," *IEEE Trans. Commun.*, vol. 60, no. 1, pp. 220–230, Jan. 2012.

[23] M. J. Neely, "Stochastic network optimization with application to communication and queueing systems," in *Synthesis Lectures on Communication Networks*, vol. 3. San Rafael, CA, USA: Morgan & Claypool, 2010, pp. 1–211.

[24] J. Yang, Q. Yang, Z. Shen, and K. S. Kwak, "Suboptimal online resource allocation in hybrid energy supplied OFDMA cellular networks," *IEEE Commun. Lett.*, vol. 20, no. 8, pp. 1639–1642, Aug. 2016.

[25] X. Wang, T. Ma, R. Zhang, and X. Zhou, "Stochastic online control for energy-harvesting wireless networks with battery imperfections," *IEEE Trans. Wireless Commun.*, vol. 15, no. 12, pp. 8437–8448, Dec. 2016.

[26] *Cisco Visual Networking Index: Global Mobile Data Traffic Forecast Update, 2013-2018*, CISCO, San Jose, CA, USA, 2014.

[27] *Dynamic Adaptive Streaming Over HTTP (DASH)—Part 1: Media Presentation Description and Segment Formats*, ISO/IEC Standard TS 26.247 V11.2.0, Apr. 2012.

[28] M. A. Hoque, M. Siekkinen, and J. K. Nurminen, "Energy efficient multimedia streaming to mobile devices—A survey," *IEEE Commun. Surveys Tuts.*, vol. 16, no. 1, pp. 579–597, 1st Quart., 2014.

[29] R. Guruprasad and S. Dey, "Rate adaptation and base station reconfiguration for battery efficient video download," in *Proc. IEEE WCNC*, Shanghai, China, Apr. 2013, pp. 339–344.

[30] H. Abou-Zeid, H. S. Hassanein, and S. Valentin, "Energy-efficient adaptive video transmission: Exploiting rate predictions in wireless networks," *IEEE Trans. Veh. Technol.*, vol. 63, no. 5, pp. 2013–2026, Jun. 2014.

[31] A. Kwasinski and A. Kwasinski, “Traffic management for sustainable LTE networks,” in *Proc. IEEE GLOBECOM*, Austin, TX, USA, 2014, pp. 2618–2623.
[32] L. Huang and M. J. Neely, “Utility optimal scheduling in energy harvesting networks,” *IEEE/ACM Trans. Netw.*, vol. 21, no. 4, pp. 1117–1130, Aug. 2013.
[33] Y.-F. Liu and Y.-H. Dai, “On the complexity of joint subcarrier and power allocation for multi-user OFDMA systems,” *IEEE Trans. Signal Process.*, vol. 62, no. 3, pp. 583–596, Feb. 2014.
[34] M. Seufert *et al.*, “A survey on quality of experience of HTTP adaptive streaming,” *IEEE Commun. Surveys Tuts.*, vol. 17, no. 1, pp. 469–492, 1st Quart., 2015.
[35] F. P. Kelly, A. Maulloo, and D. K. H. Tan, “Rate control for communication networks: Shadow prices, proportional fairness and stability,” *J. Oper. Res. Soc.*, vol. 49, no. 3, pp. 237–252, 1998.
[36] O. Arnold, F. Richter, G. Fettweis, and O. Blume, “Power consumption modeling of different base station types in heterogeneous cellular networks,” in *Proc. IEEE Future Netw. Mobile Summit*, 2010, pp. 1–8.
[37] *Physical Channels and Modulation, Evolved Universal Terrestrial Radio Access (E-UTRA)*, 3GPP TS Standard 36.211, 2011.
[38] H. Sun, B. Wang, R. Kapoor, S. Sambhwani, and M. Scipione, “Introducing heterogeneous networks in HSPA,” in *Proc. IEEE Int. Conf. Commun. (ICC)*, Ottawa, ON, Canada, 2012, pp. 6045–6050.

Po-Han Chiang (S’14) received the B.S. and M.S. degrees in electrical and communication engineering from National Taiwan University, Taipei, Taiwan, in 2011 and 2013, respectively. He is currently pursuing the Ph.D. degree in computer engineering with the University of California at San Diego, La Jolla, CA, USA. His research interests include energy harvesting cellular systems, stochastic optimization, and machine learning application.

Ranjini B. Guruprasad is currently a Research Staff Member with IBM Research Laboratory, India. Her research is focused on big data analytics with specific focus of algorithms that fuse local sensor, and satellite data and weather data to generate precision agriculture advisories and monitor water quality of large water bodies.

Sujit Dey (S’03–M’91–SM’03–F’14) is a Professor with the Department of Electrical and Computer Engineering, University of California at San Diego (UCSD), where he heads the Mobile Systems Design Laboratory, which is developing innovative technologies in mobile cloud computing, adaptive multimedia and networking, green computing and communications, and predictive and prescriptive analytics to enable future applications in connected health, immersive multimedia, smart cities, and smart transportation. He is the Director of the Center for Wireless Communications and the Institute for the Global Entrepreneur, UCSD. In 2017, he was appointed as the Jacobs Family Chair in Engineering Management Leadership.

He received the Ph.D. degree in computer science from Duke University in 1991. In 1997, he joined UCSD. He served as the Faculty Director of the von Liebig Entrepreneurism Center from 2013 to 2015, and as the Chief Scientist of Mobile Networks, Allot Communications from 2012 to 2013. He served as the Chair of the Advisory Board of Zyray Wireless till its acquisition by Broadcom in 2004, and as an advisor to multiple companies including ST Microelectronics and NEC. He founded Ortiva Wireless in 2004, where he served as its founding CEO and later as CTO and Chief Technologist till its acquisition by Allot Communications in 2012. He was a Senior Research Staff Member with NEC C&C Research Laboratories, Princeton, NJ, USA.

Dr. Dey was a recipient of six IEEE/ACM Best Paper Awards and has chaired multiple IEEE conferences and workshops. He has co-authored over 250 publications, and a book on low-power design. He holds 18 U.S. and two international patents, resulting in multiple technology licensing and commercialization.